Tribology Letters (2018) 66:154
https://doi.org/10.1007/s11249-018-1112-0

ORIGINAL PAPER

An In Situ Method for Simultaneous Friction Measurements and Imaging of Interfacial Tribochemical Film Growth in Lubricated Contacts

N. N. Gosvami[1,3] · J. Ma[2,4] · R. W. Carpick[1]

Received: 9 August 2018 / Accepted: 29 October 2018 / Published online: 8 November 2018

Abstract
Tribological investigations of macroscopic lubricated sliding contacts are critical for a wide range of industrial applications including automotive engines, gears, bearings, and any other contacting surfaces in relative motion. However, the inability of existing techniques to access buried sliding interfaces with high spatial resolution inhibits the development of fundamental insights into the tribological processes at play. Here we demonstrate a novel and general in situ method, based on atomic force microscopy (AFM), in which micrometer-scale spherical probes are attached to a standard microfabricated AFM cantilever which is then slid over a substrate while immersed in a liquid lubricant. In this case, steel colloidal probes and steel substrates were used, and the contact was immersed in a commercial polyalphaolefin oil with zinc dialkyl dithiophosphate (ZDDP) additive at both room temperature and 100 °C, but the method can be used for a broad range of material combinations, lubricants, and temperatures. We demonstrate that the in situ measurements of friction force and the morphological evolution of the tribochemical films on the substrate can be simultaneously achieved with nanometer-level spatial resolution. In addition, we demonstrate that the sliding zone is readily accessible for further characterization with higher spatial resolution using standard AFM probes with nanometer-scale tip radii. Ex situ characterization of the micrometer-scale probe and the sample is also feasible, which is demonstrated by acquiring high-resolution AFM topographic imaging of the final state of the probe.

Keywords Tribochemical films · Lubricated contacts · Antiwear additives · Zinc dialkyl dithiophosphate · Atomic force microscopy

1 Introduction

Controlling and minimizing the friction and wear of sliding and rolling machine components is a crucial industrial problem as it accounts for enormous material losses, substantial energy inefficiency, safety and reliability issues, and significant environmental emission problems [1, 2]. The solution to these problems requires a deeper understanding of the fundamental mechanisms of tribological processes, which is difficult to achieve due to the complex interactions that occur at the buried multi-asperity sliding interfaces that occur in these applications. Lubricants and additives used in industrial applications for the reduction of friction and wear are typically studied by means of laboratory bench tests using various techniques, including high-frequency reciprocating rigs (HFRR) [3], pin-on-disk or other variations of tribometers, and mini-traction machines (MTM) [4]. Steel is often used for both sides of the contact in these instruments, although other materials are readily used. HFRR and

Electronic supplementary material The online version of this article (https://doi.org/10.1007/s11249-018-1112-0) contains supplementary material, which is available to authorized users.

✉ N. N. Gosvami
ngosvami@iitd.ac.in

✉ R. W. Carpick
carpick@seas.upenn.edu

[1] Department of Mechanical Engineering and Applied Mechanics, University of Pennsylvania, Philadelphia, PA 19104, USA

[2] Department of Materials Science and Engineering, University of Pennsylvania, Philadelphia, PA 19104, USA

[3] Present Address: Department of Materials Science and Engineering, Indian Institute of Technology Delhi, Hauz Khas, New Delhi 110016, India

[4] Present Address: W. L. Gore and Associates, Elkton, MD 21921, USA

pin-on-disk instruments use a macroscopic spherical probe which is slid over a flat substrate immersed under a lubricant of interest in a pure sliding mode. Speeds, loads, contact sizes, materials, and temperatures can be varied and cover a reasonably wide range which intersects a number of conditions relevant to applications. These tests provide a measure of the coefficient of friction; in addition, the amount of wear or presence of any tribochemical products and their mechanical and chemical properties are analyzed ex situ, i.e., after the sample is taken out of the fluid cell and, without any special procedures, is exposed to the ambient environment. Thus, the physical as well as the chemical properties of the sliding interface are likely to change during the ex situ characterization. The MTM allows for the study of sliding, rolling, and mixed sliding–rolling contacts [4]. In addition, a MTM can be integrated with an optical interferometer which enables monitoring any changes in the height of the probe in lubro [5], using periodic interruptions of the measurement. Several other tribometers have been designed which include in situ optical, interferometric, and holographic imaging, enabling real-time monitoring of changes in topography [6–8]. The lateral spatial resolution of these techniques is limited to a few 100 nm due to the far field diffraction limit of optical light, although the interferometric and holographic methods enable extremely high-resolution vertical measurements (nanometers). However, any optically transparent or semi-transparent materials present at the interface (e.g., certain tribofilms including those derived from ZDDP) are difficult to interpret from the interference fringes [9].

More recently, several other in situ tribometer techniques have been introduced that allow direct access of the sliding interface under lubricated conditions in a pin-on-disk tribometer [10]. One such method is based on integrating a high-magnification optical microscope with interferometry to directly observe the sliding interface [7, 8]. Other methods include in situ chemical spectroscopy (based on Raman [11, 12], infrared (IR) [13], fluorescence [14], or surface plasmon resonance [15] spectroscopy techniques), allowing the measurements of the chemical properties of the sliding interface. In addition, it is also possible to perform in situ measurements of the interface temperature during sliding [16]. However, all these spectroscopic methods require at least one counterface to be transparent to the probe used, significantly limiting the choice of materials that can be investigated. Scanning/transmission electron microscopy (SEM/TEM) techniques [17, 18] provide another method to directly observe the sliding interface with nanometer resolution. However, these techniques are not suitable for contacts immersed in oil. In addition, TEM requires the interface region to be electron transparent.

In situ tribological studies can also be performed using atomic force microscopy (AFM) which allows simultaneous imaging of the sample with nanometer spatial resolution using nanometer sharp (single-asperity) probes [19]. Conventional AFM probes are made of silicon, which can be further modified using diamond or metallic coatings. However, thin metallic coatings are often not robust enough to sustain prolonged sliding test conditions [20]. In addition, despite the simultaneous tribological measurements and imaging capabilities of the AFM, the AFM probe geometry represents a single asperity. While this can be very useful, this geometry is very different from real engineering contacts where multi-asperity contact occurs at the interface. Hence, a direct comparison between single- and multi-asperity experiments is challenging, although some work has attempted to address this [21]. Such experimental limitations and difficulties with existing techniques motivate the development of novel in situ approaches. This can allow better understanding of the tribological properties of a variety of technologically important materials in multi-asperity contact geometries under dry as well as lubricated conditions.

Here we demonstrate an AFM-based in situ approach which can be applied to a wide variety of material pairs to study multi-asperity sliding contacts under dry as well as lubricated conditions (Fig. 1a, b) with the contact immersed in lubricant oil. Microspheres attached to AFM cantilever probes have previously been used for measurement of adhesion, friction, and confined lubricant investigation [22]. Here, for the first time, we demonstrate that tribochemical reactions can be induced by sliding this probe in the presence of reactive lubricant additive molecules dispersed in the lubricant and perform simultaneous measurements of friction during sliding, as well as topographic imaging of the substrate surface within the sliding zone, enabling new insights into the tribochemical processes to be revealed. The technique can be used with many materials including technologically relevant ones such as steel, silicon, aluminum, and diamond-like carbon (DLC). Additionally, high-resolution imaging and characterization of the sliding zone and the region around it on the substrate can be performed using standard AFM probes with nanometer-scale radii without removing the sample from its oil-immersed condition in the liquid cell.

2 Experimental Methods

The steel substrates (52100 steel), heat treated to achieve 60 Rockwell C scale hardness (Heckel Tools & Mfg. Corp., Eagle, WI, USA), were polished to a mirror finish using silicon carbide polishing paper disks (180, 240, and 320 Grit), followed by polishing on a Rayon polishing cloth using a micro diamond suspension (South Bay Technologies, San Clemente, CA). The RMS roughness of the surface of the polished samples was found to be less than 1.5 nm as measured by AFM over 20 μm × 20 μm

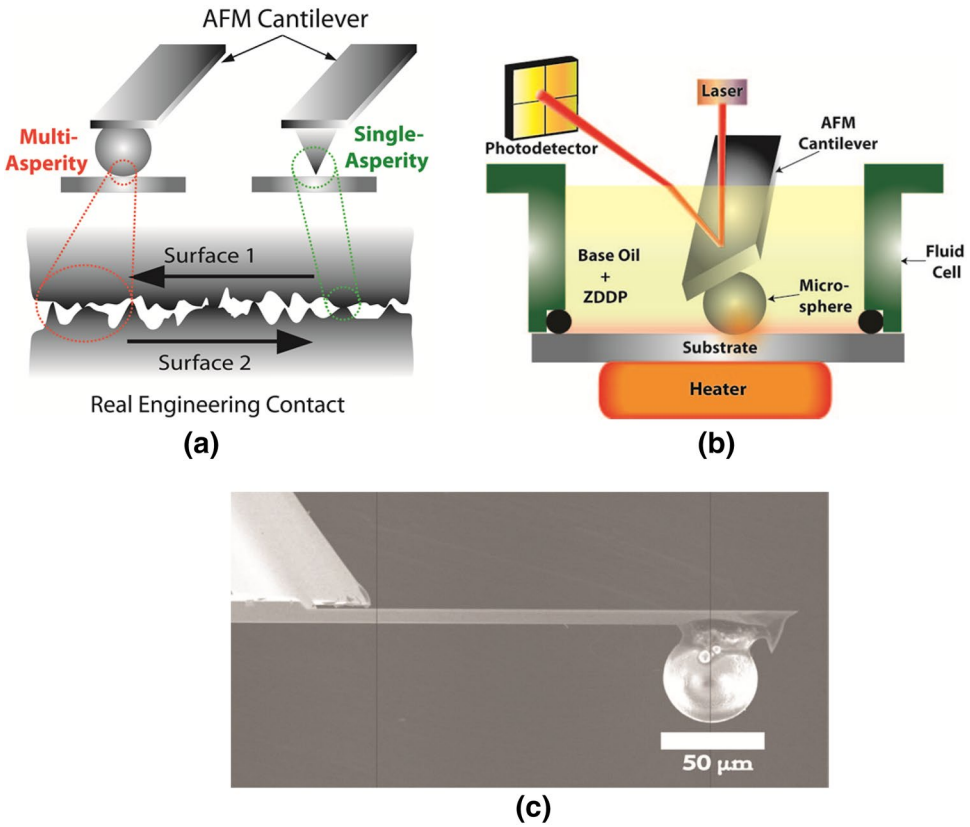

Fig. 1 **a** Schematic showing the AFM-based in situ technique where a micrometer-scale probe (in this case, a steel colloid) is slid against a substrate (in this case, 52100 steel) to investigate friction in a multi-asperity contact geometry. The probe can be switched after the experiments, and the sliding zone that was scanned can be characterized using a sharp AFM probe to provide sub-nanometer spatial resolution images. **b** Schematic of the setup for the in situ tribometer technique, which allows sliding measurements in lubricated conditions, for temperatures up to 200 °C. **c** Scanning electron micrograph of a typical cantilever where the probe is modified by gluing a steel colloid near the free end of the cantilever

area. Commercial silicon cantilevers (PPP-NCH, Nanosensors, Neuchatel, Switzerland) used in these measurements were first calibrated for their normal and lateral spring constants using the Sader method [23], and the normal force deflection sensitivity was determined from the slope of force–distance curves measured in contact [24]. This was all done in the same liquid environment as the subsequent experiments. Some were used as-is and are referred to as "sharp AFM probes." For others, steel probes were attached by gluing steel microspheres (SHS 7574 HVOF, The NanoSteel Co., Rhode Island, USA) on calibrated cantilevers using an inverted optical microscope (Alessi REL-4100A, Redwood City, CA, USA) by first applying a small quantity of a two-part epoxy (J-B Weld, Sulphur Springs, TX, USA) using a sharp tungsten wire (TGW0325, World Precision Instruments, Sarasota, FL, USA) and then placing the bead using a strand of hair [25]. The cantilevers were stored overnight in a dry N_2-purged box to allow the epoxy to fully cure. The diameters of the microspheres attached to the cantilevers were estimated either from bright field optical imaging (Olympus BX51) or using field emission scanning electron microscopy (SEM, JOEL 7500F) as shown in Fig. 1c. After gluing the bead, the normal and lateral spring constants were corrected according to ref [23, 26], respectively, in order to account for the variation in the effective length of the cantilever (the distance between the base of the cantilever to the center of the glued bead) as well as the tip height. All experiments were performed using a commercial atomic force microscope (Keysight 5500, Keysight Technologies, Santa Clara CA, USA), equipped with a sample heating plate, a liquid cell, and a temperature controller (Model 321, Lake Shore Cryotronics Inc., Westerville, OH, USA). A schematic is shown in Fig. 1b. The cantilever deflection sensitivities along the normal direction were obtained by recording force curves on the steel substrate, whereas lateral force sensitivities were obtained from the static friction versus distance curve (Fig. 2a) as described in detail in the "Results and Discussion" section. The lateral force F_L was then calibrated simply by multiplying the lateral deflection signal (in Volts) to the lateral force sensitivity (slope of the stick regime in m/V) and the cantilever stiffness (in N/m) [27, 28] as given below:

$$F_L(N) = F_L(V) \cdot S_L(\mathrm{m/V}) \cdot k_{\mathrm{Lcantilever}}(\mathrm{N/m}). \quad (1)$$

A mixture of 99 wt% base oil (SpectraSyn polyalphaolefin (PAO) 4 cSt, ExxonMobil, Houston, TX, USA) with 1 wt% zinc dialkyl dithiophosphate (ZDDP) antiwear additives (HiTEC 1656—a mixture of primary and secondary ZDDP, Afton Chemical Corp., Richmond, VA, USA) was used for all the experiments. Data analysis was performed using WSxM 5.0 software [29] and using custom Matlab routines.

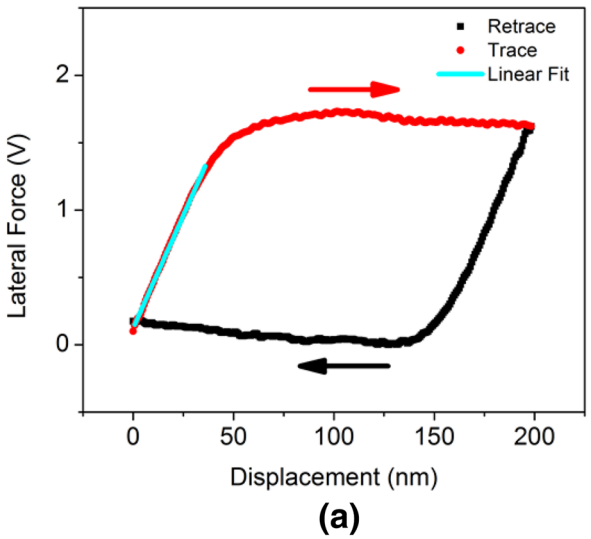

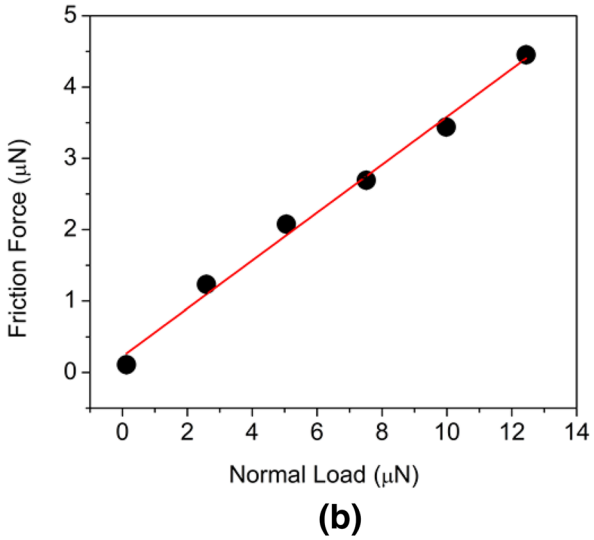

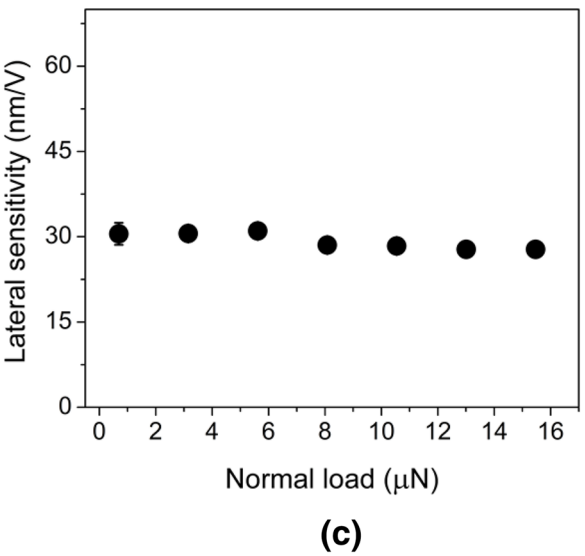

Fig. 2 **a** Friction loop acquired using a cantilever with a steel probe sliding over a polished steel substrate immersed in PAO base oil containing 1 wt% ZDDP. The friction loop shows a linear increase during the static friction portion, which then transitions to a nearly constant friction force (kinetic friction) as the lateral displacement of the sample is increased. A linear fit of the static friction regime provides the lateral force sensitivity according to Eq. 2. **b** Friction versus load measurement, performed using a 45 μm diameter steel probe sliding over a polished steel substrate. The data fit well to a linear function. **c** The lateral sensitivity of an AFM cantilever with a steel probe, acquired by measuring the slope of the linear static friction regime of the friction loop. The lateral sensitivity is constant for a large range of normal loads, indicating no observable effect on the contact stiffness

3 Results and Discussion

We first demonstrate the feasibility of micrometer-scale steel probes mounted on AFM cantilevers to measure frictional forces for steel-on-steel contacts under lubricated conditions. This first requires the calibration of the lateral force sensitivity of the steel probe cantilever which can be deduced from friction loops, obtained by measuring the lateral deflection signal of the cantilever during the forward and reverse sliding directions. Figure 2a shows a lateral force versus displacement curve obtained before starting a sliding experiment using a fresh steel probe sliding on a freshly polished steel substrate, immersed in the lubricant oil. The lateral force versus displacement curve shows two distinct regimes: a linear increase of lateral force with lateral displacement in the sticking regime (static friction regime, i.e., before slip of the probe across the surface occurs while the base of the cantilever is being displaced by the piezo scanner), followed by an approximately constant lateral force versus lateral displacement, i.e., continuous sliding of the probe occurring in the second regime (kinetic friction regime). We note that the transition between the sticking and sliding phase is not as sharp as often seen in single-asperity measurements; the reasons for this are not clear, but is likely due to a reduction of contact stiffness due to partial slip [30]; such behavior has been reported in other colloidal probe measurements [27, 31].

The lateral force versus displacement curve in the first regime can be fit to a linear function and the slope of the fit line provides the total stiffness k_{total} [32] as given below:

$$\frac{1}{k_{\text{total}}} = \frac{1}{k_{\text{L,cantilever}}} + \frac{1}{k_{\text{contact}}}, \tag{2}$$

where k_{total} is the total stiffness measured in the static friction regime (i.e., the slope of the linear fit); k_{contact} is the lateral contact stiffness; and $k_{\text{L,cantilever}}$ is the lateral stiffness of the AFM cantilever. Lateral contact stiffness k_{contact} scales linearly with the true contact radius for a single asperity, and but is a more complex function for a multi-asperity contact. However, if the lateral contact stiffness

is large in comparison to the cantilever lateral stiffness ($k_{L,cantilever} << k_{contact}$) then $k_{total} \approx k_{L,cantilever}$ and the slope of the lateral force versus displacement will be independent of the normal load. This is indeed observed in our measurements as shown in Fig. 2c, where the variation in the measured lateral force sensitivity is < 5% for more than one order of magnitude variation in the normal load (0.7–15.5 μN).

We now demonstrate the ability of the steel probe to image the topography of the substrate surface as well as perform simultaneous friction measurements. Figure 3a shows an AFM topographic image of a typical polished steel substrate, acquired using a sharp silicon AFM probe at a load of 130 nN. Figure 3b shows the topographic image of the same substrate acquired using a steel probe at a load of 200 nN. Both the images in Fig. 3 were acquired in air, before filling the AFM liquid cell with the lubricant. Interestingly, the morphology of the steel substrate is nearly equally well resolved using most of the steel probes used in our experiments. The resolution is certainly far better than what one would expect using the full radius of the colloidal probe to calculate the contact diameter, which would be 60 nm using a load of 200 nN, the elastic properties of steel, and the probe radius of 22.5 μm. We attribute this to the roughness of the steel probe which has features down to the nanometer scale. Thus, near the region of the probe that is closest to the substrate, the image resolution strongly suggests that a small asperity protrudes more compared to others, and thus contributes most to the topographic image. Of course, this geometry would limit the probing of deeper trenches or sidewall features to a greater extent than for the sharp probe. As seen further below, high spatial resolution was also observed when imaging in the lubricant with the colloidal probe.

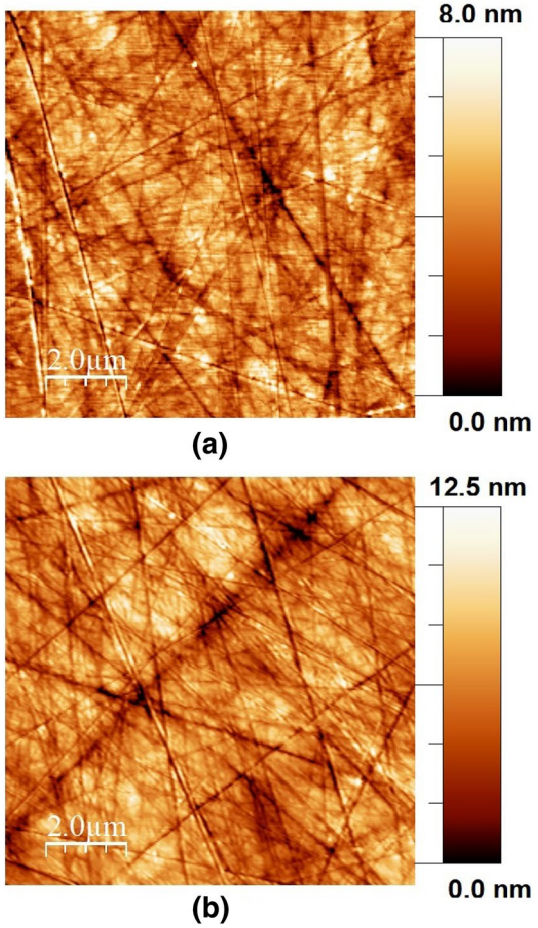

Fig. 3 **a** 10 μm × 10 μm AFM topographic image of a polished steel substrate, acquired using a sharp AFM tip. **b** 10 μm × 10 μm AFM topographic image of a polished steel substrate, acquired using a 45-μm diameter steel probe mounted on a cantilever

The roughness of the same steel probe was directly imaged by mounting it as a sample in the AFM, with the steel probe facing up. Then, a sharp AFM probe is optically aligned right above the upward-facing steel probe surface in the AFM and brought into contact with it. A topographic image of one of the unused steel probes is shown in Fig. 4a and b. The RMS roughness of a 10 μm × 10 μm area is < 2 nm, and the line profile in Fig. 4b clearly shows that nanoscale asperities are present on the probe surface. A simple estimate using the Hertz model for the overall elastic deformation of a smooth steel sphere at the applied load of 200 nN gives 0.04 nm, which is more than an order of magnitude smaller than the heights of the bumps shown in Fig. 4. This suggests these bumps may not be deformed enough to lead to a multi-asperity contact. Indeed, the image quality we see also supports only a single-asperity contact. The ability to perform high-resolution imaging of the steel probe surface also enables measurement of any wear, contamination, or tribofilm growth occurring on the steel probe within and around the contact zone. Note that one also needs to be careful during imaging of the colloid surface with a sharp tip as the contact zone is not at the bottom due to the tilt of the cantilever (~ 15° for this instrument) which was mounted to the cantilever holder during the experiment.

For the measurements of the coefficient of friction (μ), it needs to be determined if the friction force varies linearly with the normal load according to the Amontons' first law as given below:

$$F_L = \mu F_N. \quad (3)$$

In order to verify the relationship in Eq. 3, friction force was measured for a range of normal loads under PAO containing 1 wt% ZDDP at room temperature. A linear relationship between friction force and normal load is observed as shown in Fig. 2b, confirming that the coefficient of friction can be measured for normal loads up to at least 15 μN.

Friction measurements were then performed in different locations and the morphology of the substrate's surface was continuously monitored (an example is shown in Fig. 5). A normal load of 12 μN was used, which corresponds to a

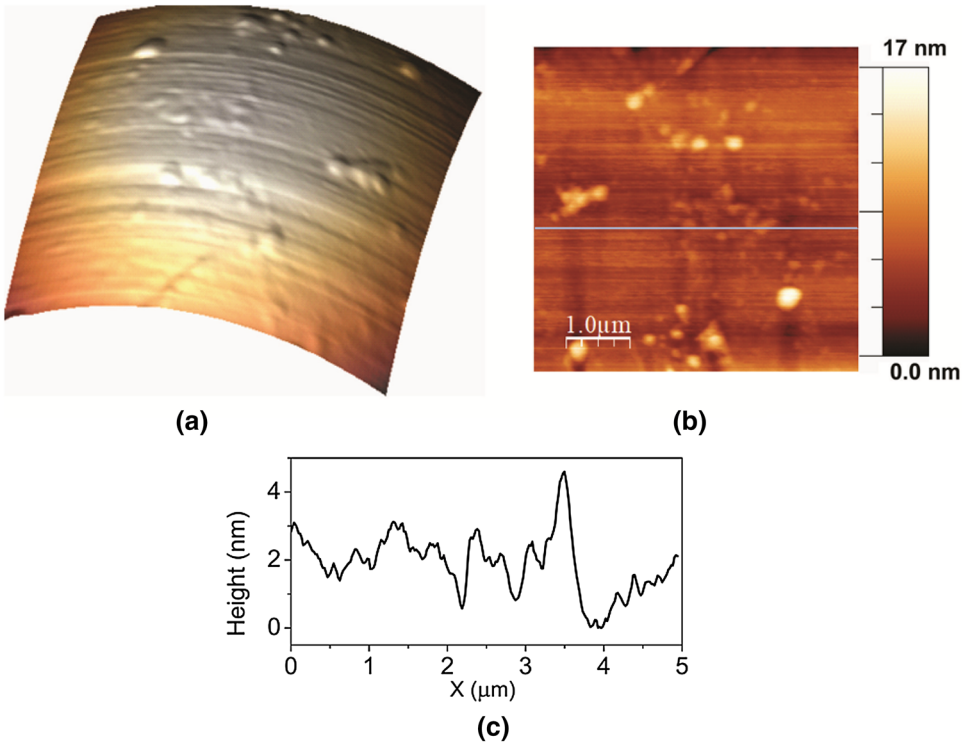

Fig. 4 **a** 5 μm × 5 μm topographic image of the surface of a steel colloid probe acquired using a sharp AFM tip. **b** Topographic image of **a** after flattening to reveal surface features. **c** Line profile depicting the surface roughness of the steel probe surface

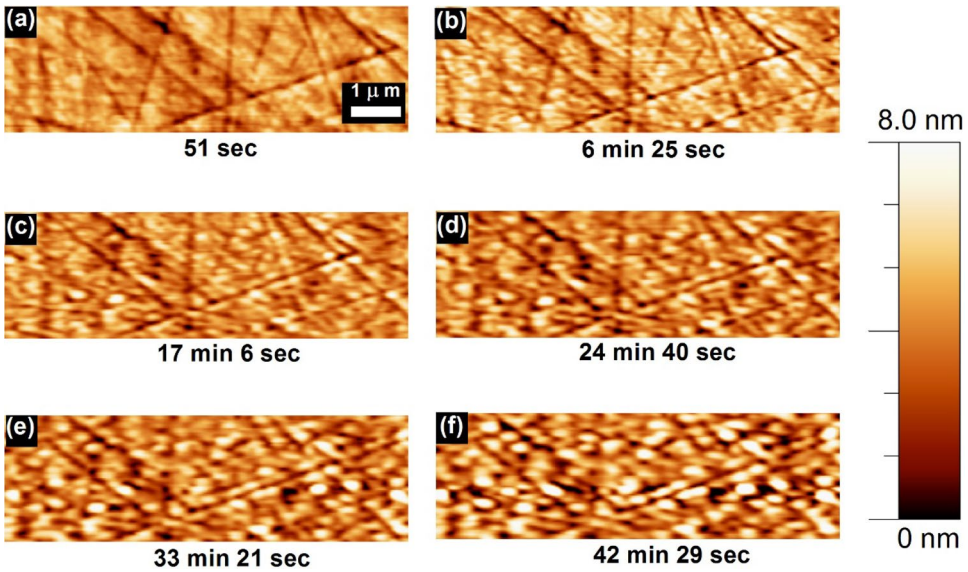

Fig. 5 **a**–**f** 8.0 μm × 2.5 μm AFM deflection images of the raster scan region where the in situ growth of the tribofilm is monitored using a steel colloid probe at 100 °C. Scratches on the polished steel surfaces as well as the nucleation and growth of the ZDDP islands can be easily resolved. A movie showing this process is provided in the Supplementary Material

mean Hertzian pressure of ~ 0.25 GPa. The sliding speed was 100 μm/s over a scan width of 8 μm, corresponding to a scan rate of 12.5 Hz. The experiments were performed at room temperature in the lubricant. The resulting coefficient of friction is plotted for measurements performed at room temperature as well as at elevated temperatures of 100 °C (Fig. 6). The room temperature data show higher friction as well as larger fluctuations in the friction force for the first ~ 700 sliding cycles, and then it reduces. This transient behavior could be indicative of a run-in process where wear of both the substrate and the colloidal probe occurs due to high localized stresses acting at the contacting asperities at the given load.

The measured steady-state coefficient of friction values of ~ 0.3 are approximately a factor of two higher than the values measured using macroscale pin-on-disk [33] as well as the MTM [34] techniques for steel-on-steel in PAO with 1 wt% ZDDP. The discrepancy is not necessarily surprising; the contact mechanics behavior for rough surfaces will be different for macroscale versus microscale experiments.

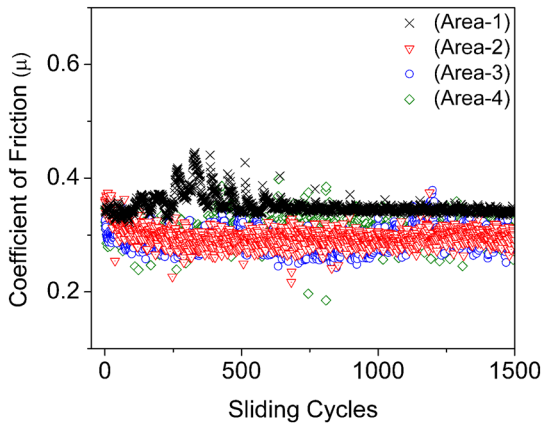

Fig. 6 Coefficient of friction (μ) versus sliding cycles for a steel colloid probe sliding on a polished steel substrate in a lubricated contact (PAO containing 1 wt% ZDDP). Experiments performed in four different regions are shown, where the measurement in Area 1 was performed at room temperature, and the other measurements (Areas 2–4) were performed at 100 °C

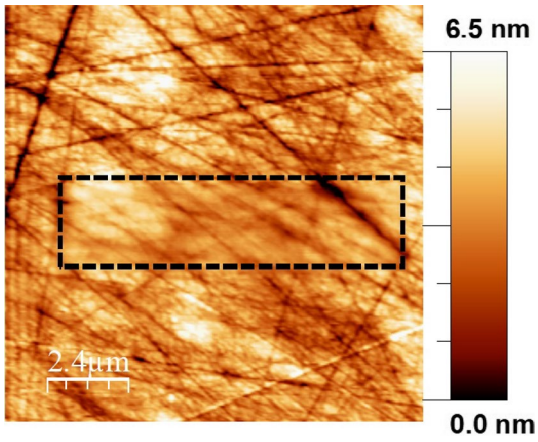

Fig. 7 12 μm × 12 μm AFM topography images of a polished steel surface, obtained using a 45.0-μm diameter steel probe attached to an AFM cantilever. The image was acquired after 200 cycles of raster scan in the central 8.0 μm × 2.5 μm region (dotted rectangle) at room temperature. Scratches on the polished steel surfaces as well as the morphological changes due to continuous sliding at high normal loads (12.5 μN) in the central region are readily resolved. The simultaneously measured values of coefficient of friction are presented in Fig. 6

In addition, we are using much lower sliding speeds in the AFM experiments, namely, 50–200 μm/s, compared to 100–400 mm/s for the larger scale using pin-on-disk [33] and MTM [34] experiments. The lower AFM sliding speeds will correspond to the higher friction regime on the Stribeck curve, likely in the boundary lubrication regime. Another possible cause is the difference in mean (Hertzian) contact pressure, which is somewhat less in our experiments (approximately, 0.2 GPa here vs. 0.9 GPa in [34]).

Since this method allows us to directly image the surface, an image was acquired of the surrounding region using a much reduced load (no more than 100 nN) to avoid further modification of the substrate, after sliding the probe at room temperature for 200 cycles (Fig. 7). The image clearly shows changes in the surface morphology within the sliding zone. The scanned region (indicated by the dotted rectangle) has undergone mild wear and accordingly is smoother with an RMS roughness of 0.9 nm compared to 1.2 nm for the unworn region (both measured over an area of 20 μm^2), confirming that mild wear has occurred.

No growth of any sliding-induced material transfer or tribochemical film was observed within the timeframe of these room temperature experiments. However, nucleation and growth of the antiwear tribofilms were observed within the sliding zone upon continuous sliding at elevated temperatures (~ 100 °C). Figure 5 shows a set of images from the series of topographic images recorded in situ during sliding at 100 °C, which clearly shows nucleation of discrete islands of the tribofilm within the sliding zone. The full series of images was converted into a movie to visualize the in situ growth of the tribofilm, as shown in Supplementary Materials Movie 1. We observe that during initial sliding, several island-like features grow near scratches on the steel substrate. This may be explained by the stress-induced increase in growth rate of ZDDP-derived tribofilms [35], since the stresses will be higher when the probe is sliding over the edges of scratches due to significant reduction in contact area at such locations. Most strikingly, the morphology of the tribofilm (as shown in the zoomed-out topographic image shown in Fig. 8) matches qualitatively well with the tribofilms produced in single-asperity contact on smooth iron films as well as on silicon substrates [35], which supports a stress-assisted, thermally activated process for the

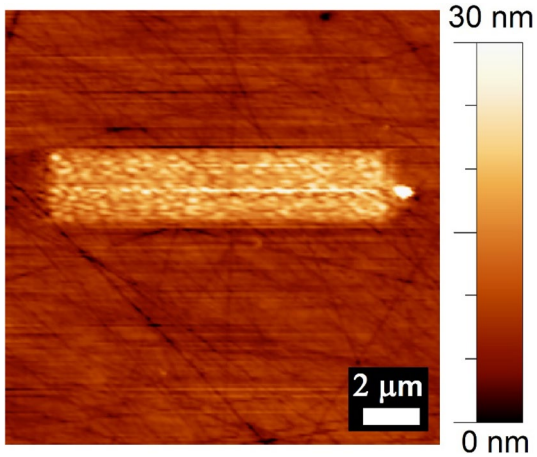

Fig. 8 15 μm × 15 μm AFM topography of the steel substrate acquired using a sharp probe. The in situ tribofilm, generated in a 8.0 μm × 2.5 μm region, is clearly resolved

tribofilm growth, as described well by Arrhenius reaction rate theory [35]. We do not observe a transient increase in coefficient of friction during the initial sliding cycles, unlike that typically observed in macroscale experiments [36]. In such experiments, loads of several Newtons, corresponding to a mean Hertzian contact pressure of ~ 1.0 GPa were used [37], which leads to significant wear during the initial sliding cycles due to considerably higher localized asperity-level contact pressures. This observation suggests insignificant wear of the substrate as well as the tribofilm occurring during our sliding tests.

The tribofilms generated using colloidal probes can be easily located optically and can be further characterized using sharp AFM probes. An example of a similar tribofilm generated and imaged in situ using a steel probe is shown in Fig. 9a. The same tribofilm is then imaged using a sharp probe as shown in Fig. 9b. The sharp probe reproduces the image obtained using the steel probe cantilever but with enhanced resolution and this validates that the tribofilm can be easily located for further investigations using other AFM modes. The volume of the tribofilm obtained by each probe was calculated from the AFM images using a MATLAB routine; the uncertainty is calculated by the standard deviation of at least five independent calculations of the volume of the tribofilm. The tribofilm volume calculated from the image obtained using the steel probe is 2.12 ± 0.02 μm^3, and from the image obtained using sharp probe is 2.51 ± 0.02 μm^3. This suggests that the quantitative topography mapping of a tribofilm using steel probe is reasonably comparable to that of a sharp cantilever. The lower volume measured by the blunt probe is clearly unexpected given the larger contact area of the blunt probe (even accounting for a sharper asperity that terminates it and is responsible for imaging). As shown in the topographic line profiles of Fig. 9a and b, the height measured by the blunt probe is significantly lower, which is what produces the lower tribofilm volume. One possible explanation is that this arises from the higher load used with the stiffer cantilever using the colloidal probe (200 nN) in comparison to the low forces used with the low stiffness cantilever with the sharp probe (< 10 nN). Higher imaging load could lead to compression of the compliant tribofilm resulting in lower measured height. Quantifying this without knowing the depth-dependent modulus is not possible, but low moduli (< 30 GPa) have been reported for ZDDP tribofilms previously [38]; further work is required to understand this effect. Clearly, low loads are preferable for resolving tribofilm volumes accurately.

Note that the tribofilm is generated over a rather large area (20 μm^2) and exhibits tribofilm islands with lateral features of sizes 100 nm. Thus, even a large colloidal probe is able to accurately image features of this scale. The agreement may not be so good if the tribofilm has features with significant height variations at smaller lateral sizes.

It is also feasible to characterize the topography of steel probes after the sliding tests. An example is shown in Fig. S1 where the steel probe that was used for the in situ experiments (Figs. 5, 6, 7, 8) is imaged using a sharp AFM probe before and after the sliding test. Fig. S1b clearly reveals the flattened region where wear occurred during sliding and we do not observe buildup of any significant amount of tribofilm within this region. This suggests that the degree of growth of tribofilm on the probe is low. This may be due to the fact that the probe is continuously sliding over the substrate surface,

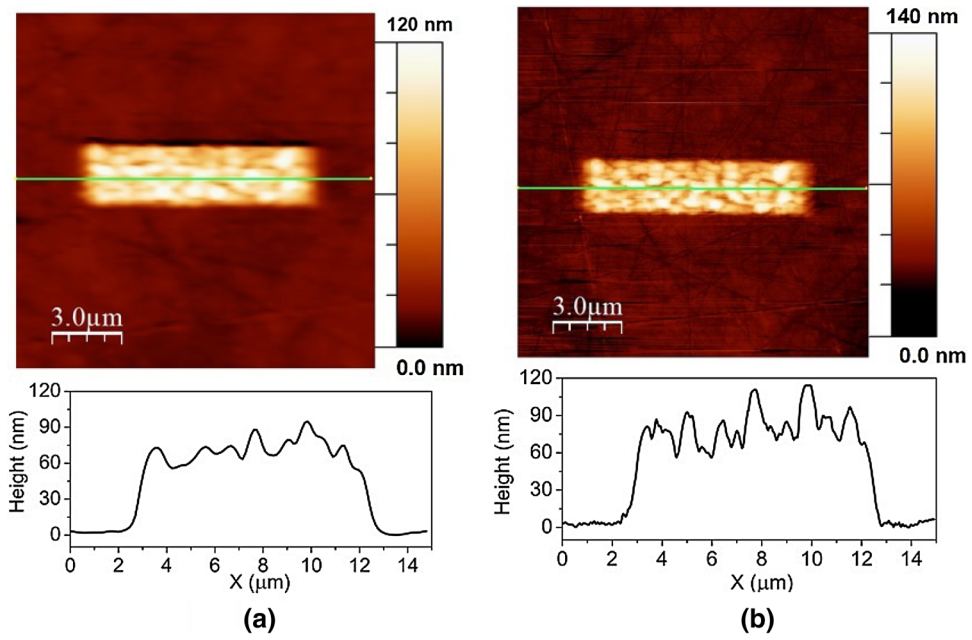

Fig. 9 **a** 15 μm × 15 μm AFM topography image of the steel substrate acquired using a steel probe cantilever, revealing the in situ tribofilm generated in a 8.0 μm × 2.5 μm central region. **b** 15 μm × 15 μm AFM topography of the same region as in (**a**) using a sharp silicon probe cantilever, revealing the in situ tribofilm generated in a 8.0 μm × 2.5 μm central region. Line profile shown below of the lines indicated in (**a** & **b**) showing details of the tribofilm morphology

resulting in the removal of any deposited material on the probe surface as well as wear of the probe surface itself.

The nanoscale mechanical properties of tribofilms generated under these well-controlled conditions are currently being investigated, and the results will be published separately.

In conclusion, we demonstrate a novel method to perform in situ tribological investigations of lubricated contacts. The experiments performed using a steel probe sliding over a polished steel substrate in ZDDP containing PAO base oil reveal that the coefficient of friction as well as the morphological evolution of the tribochemical films can be monitored in situ. In addition, this method allows the use of a sharp (nanometer-scale radius) AFM probe to measure topography as well as other physical properties of the regions of interest, e.g., in the sliding zone, without removing the sample out of the fluid cell. This provides an important complement to macroscopic tribometer tests, where the sliding interface is buried during the test and ex situ tests may introduce changes in the properties of the sliding zone. Another significant advantage of this method is that it can be applied to a wide variety of material systems. In addition, this method is compatible with approaches that use tribochemical reactions at surfaces to form patterns, as demonstrated in a recent publication [39].

Notwithstanding unique advantages, it is also important to note the limitations of this technique. One limitation is the small contact size, which despite being multi-asperity, is orders of magnitude smaller than practical macroscale engineering contacts. In addition, as this is an AFM-based technique, the sliding speeds are on the order of a few micrometers per second, significantly smaller than typical values for engineering applications and the wider speed range that can be achieved using conventional macroscopic tribometers, i.e., mm/sec to m/sec. The slow sliding speeds also limit the lubrication regimes that can be explored using this method, i.e., using this technique, we are operating essentially in boundary lubrication regime. However, atomic force microscopy technique is improving substantially, and scanning speeds on the order of mm/sec-cm/sec have been recently demonstrated [40–42] which can potentially allow exploring various lubrication regimes, similar to the existing tribometers. Results pursuing these approaches will be presented in a future publication.

Acknowledgements This work was supported by the National Science Foundation under grants CMMI-1200019 and CMMI-1728360, and the University of Pennsylvania through the School of Engineering and Applied Sciences, and the Vagelos Integrated Program in Energy Research (VIPER). The authors acknowledge the use of University of Pennsylvania Nano/Bio Interface Center Facilities and the Nanoscale Characterization Facility in the Singh Center for Nanotechnology. We thank Mr. Qizhan Tam for MATLAB analysis. The authors gratefully acknowledge helpful discussions with Prof. Andrew Jackson.

References

1. Jones, M.H., Scott, D.: Industrial Tribology: The Practical Aspects of Friction, Lubrication and Wear. Elsevier, Amsterdam (1983)
2. Carpick, R.W., Jackson, A., Sawyer, W.G., Argibay, N., Lee, P., Garcia, A.P., et al.: Tribology Opportunities for Enhancing America's Energy Efficiency: A Report to the Advanced. Research Projects Agency-Energy at the U.S. Department of Energy, Place (2017)
3. McQueen, J., Gao, H., Black, E., Gangopadhyay, A., Jensen, R.: Friction and wear of tribofilms formed by zinc dialkyl dithiophosphate antiwear additive in low viscosity engine oils. Tribol. Int. **38**, 289–297 (2005)
4. Taylor, L., Dratva, A., Spikes, H.: Friction and wear behavior of zinc dialkyldithiophosphate additive. Tribol. Trans. **43**, 469–479 (2000)
5. Fujita, H., Spikes, H. The formation of zinc dithiophosphate antiwear films. Proc. Inst. Mech. Eng.: Part J. J. Eng. Tribol. **218**:265–278 (2004)
6. Ovcharenko, A., Halperin, G., Etsion, I., Varenberg, M. : A novel test rig for in situ and real time optical measurement of the contact area evolution during pre-sliding of a spherical contact. Tribol. Lett. **23**, 55–63 (2006)
7. Krick, B.A., Vail, J.R., Persson, B.N., Sawyer, W.G.: Optical in situ micro tribometer for analysis of real contact area for contact mechanics, adhesion, and sliding experiments. Tribol. Lett. **45**, 185–194 (2012)
8. Sheasby, J., Caughlin, T., Habeeb, J.: Observation of the antiwear activity of zinc dialkyldithiophosphate additives. Wear **150**, 247–257 (1991)
9. Benedet, J., Green, J.H., Lamb, G.D., Spikes, H.A.: Spurious mild wear measurement using white light interference microscopy in the presence of antiwear films. Tribol. Trans. **52**, 841–846 (2009)
10. Sawyer, W.G., Wahl, K.J.: Accessing inaccessible interfaces: in situ approaches to materials tribology. MRS Bull. **33**, 1145–1150 (2008)
11. Cheong, C.U.A., Stair, P.C.: In situ studies of the lubricant chemistry and frictional properties of perfluoropolyalkyl ethers at a sliding contact. Tribol. Lett. **10**, 117–126 (2001)
12. Scharf, T., Singer, I.: Monitoring transfer films and friction instabilities with in situ Raman tribometry. Tribol. Lett. **14**, 3–8 (2003)
13. Mangolini, F., Rossi, A., Spencer, N.D.: In situ attenuated total reflection (ATR/FT-IR) tribometry: a powerful tool for investigating tribochemistry at the lubricant–substrate interface. Tribol. Lett. **45**, 207–218 (2012)
14. Bae, S.C., Wong, J.S., Kim, M., Jiang, S., Hong, L., Granick, S.: Using light to study boundary lubrication: spectroscopic study of confined fluids. Philos. Trans. Royal Soc. of Lond. A: Math., Phys. Eng. Sci. **366**, 1443–1454 (2008)
15. Krick, B.A., Hahn, D.W., Sawyer, W.G.: Plasmonic diagnostics for tribology: in situ observations using surface plasmon resonance in combination with surface-enhanced Raman spectroscopy. Tribol. Lett. **49**, 95–102 (2013)
16. Rowe, K.G., Bennett, A.I., Krick, B.A., Sawyer, W.G.: In situ thermal measurements of sliding contacts. Tribol. Int. **62**, 208–214 (2013)
17. Murarash, B., Varenberg, M.: Tribometer for in situ scanning electron microscopy of microstructured contacts. Tribol. Lett. **41**, 319–323 (2011)
18. Marks, L.D., Warren, O.L., Minor, A.M., Merkle, A.P.: Tribology in full view. MRS Bull. **33**, 1168–1173 (2008)
19. Carpick, R.W., Salmeron, M.: Scratching the surface: fundamental investigations of tribology with atomic force microscopy. Chem. Rev. **97**, 1163–1194 (1997)

20. Lantz, M., O'shea, S., Welland, M.: Simultaneous force and conduction measurements in atomic force microscopy. Phys. Rev. B **56**, 15345 (1997)
21. Li, Q., Kim, K.-S. Micromechanics of friction: effects of nanometre-scale roughness. Proc. Royal Soc. A: Math., Phys. Eng. Sci. **464**:1319–1343 (2008)
22. Gebbie, M.A., Smith, A.M., Dobbs, H.A., Warr, G.G., Banquy, X., Valtiner, M., et al.: Long range electrostatic forces in ionic liquids. Chem. Commun. **53**, 1214–1224 (2017)
23. Green, C.P., Lioe, H., Cleveland, J.P., Proksch, R., Mulvaney, P., Sader, J.E.: Normal and torsional spring constants of atomic force microscope cantilevers. Rev. Sci. Instrum. **75**, 1988–1996 (2004)
24. Cappella, B., Dietler, G.: Force-distance curves by atomic force microscopy. Surf. Sci. Rep. **34**, 1–104 (1999)
25. Florin, E.L., Radmacher, M., Fleck, B., Gaub, H.E.: Atomic force microscope with magnetic force modulation. Rev. Sci. Instrum. **65**, 639–643 (1994)
26. Sader, J.E., Larson, I., Mulvaney, P., White, L.R.: Method for the calibration of atomic force microscope cantilevers. Rev. Sci. Instrum. **66**, 3789–3798 (1995)
27. Cain, R.G., Biggs, S., Page, N.W.: Force calibration in lateral force microscopy. J. Colloid Interface Sci. **227**, 55–65 (2000)
28. Chung, K.-H., Pratt, J.R., Reitsma, M.G.: Lateral force calibration: accurate procedures for colloidal probe friction measurements in atomic force microscopy. Langmuir **26**, 1386–1394 (2009)
29. Horcas, I., Fernández, R., Gomez-Rodriguez, J., Colchero, J., Gómez-Herrero, J., Baro, A.: WSXM: a software for scanning probe microscopy and a tool for nanotechnology. Rev. Sci. Instrum. **78**, 013705 (2007)
30. Mindlin, R.: Compliance of elastic bodies in contact. J. Appl. Mech. Trans. ASME **16**, 259–268 (1949)
31. Mazeran, P.-E., Loubet, J.-L.: Normal and lateral modulation with a scanning force microscope, an analysis: implication in quantitative elastic and friction imaging. Tribol. Lett. **7**, 199–212 (1999)
32. Carpick, R.W., Ogletree, D., Salmeron, M.: Lateral stiffness: a new nanomechanical measurement for the determination of shear strengths with friction force microscopy. Appl. Phys. Lett. **70**, 1548–1550 (1997)
33. Gao, H., McQueen, J., Black, E., Gangopadhyay, A., Jensen, R.: Reduced phosphorus concentration effects on tribological performance of passenger car engine oils. Tribol. Trans. **47**, 200–207 (2004)
34. Miklozic, K.T., Forbus, T.R., Spikes, H.A.: Performance of friction modifiers on ZDDP-generated surfaces. Tribol. Trans. **50**, 328–335 (2007)
35. Gosvami, N., Bares, J., Mangolini, F., Konicek, A., Yablon, D., Carpick, R.: Mechanisms of antiwear tribofilm growth revealed in situ by single-asperity sliding contacts. Science **348**, 102–106 (2015)
36. Kim, B., Mourhatch, R., Aswath, P.B.: Properties of tribofilms formed with ashless dithiophosphate and zinc dialkyl dithiophosphate under extreme pressure conditions. Wear **268**, 579–591 (2010)
37. Fujita, H., Glovnea, R., Spikes, H.: Study of zinc dialkydithiophosphate antiwear film formation and removal processes, part I: Experimental. Tribol. Trans. **48**, 558–566 (2005)
38. Bec, S., Tonck, A., Georges, J.-M., Coy, R., Bell, J., Roper, G.: Relationship between mechanical properties and structures of zinc dithiophosphate anti–wear films. Proceedings of the Royal Society of London A: Mathematical, Physical and Engineering Sciences, pp. 4181–4203. The Royal Society, Place The Royal Society (1999)
39. Khare, H.S., Gosvami, N.N., Lahouij, I., Milne, Z.B., McClimon, J.B., Carpick, R.W.: Nanotribological Printing: A Nanoscale Additive Manufacturing Method. Submitted (2018)
40. Bosse, J.L., Lee, S., Andersen, A.S., Sutherland, D.S., Huey, B.D.: High speed friction microscopy and nanoscale friction coefficient mapping. Meas. Sci. Technol. **25**, 115401 (2014)
41. Ren, J., Zou, Q.: High-speed adaptive contact-mode atomic force microscopy imaging with near-minimum-force. Rev. Sci. Instrum. **85**, 073706 (2014)
42. Ren, J., Zou, Q., Li, B., Lin, Z.: High-speed atomic force microscope imaging: adaptive multiloop mode. Phys. Rev. E **90**, 012405 (2014)